sustainability

MDPI

Article

Sustainable Non-Cooperative User Detection Techniques in 5G Communications for Smart City Users

Shayla Islam [1], Anil Kumar Budati [1,*], Mohammad Kamrul Hasan [2], Hima Bindu Valiveti [3] and Sridhar Reddy Vulupala [4]

[1] Institute of Computer Science and Digital Innovation, UCSI University, Kuala Lumpur 56000, Malaysia
[2] Center for Cyber Security, UKM University, Bangi 43600, Malaysia
[3] Department of ECE, Gokaraju Rangaraju Institute of Engineering & Technology (GRIET), Hyderabad 500090, India
[4] Department of IT, Vignana Bharathi Institute of Technology, Hyderabad 501301, India
* Correspondence: anilbudati@gmail.com

Abstract: The 4G network is not sufficient for achieving the high data requirements of smart city users. The 5G network intends to meet these requirements and overcome other application issues, such as fast data transmission, video buffering, and coverage issues, providing excellent mobile data services to smart city users. To allocate a channel or spectrum to a smart city user for error-free transmission with low latency, the accurate information of the spectrum should be detected. In this study, we determined the range of non-cooperative detection techniques, such as matched filter detection with inverse covariance approach (MFDI), cyclostationary feature detection with inverse covariance approach (CFDI), and hybrid filter detection with inverse covariance approach (HFDI); based on the results of these methods, we provided highly accurate spectrum information for smart city users, enabling sustainable development. To evaluate the performance of the proposed detection techniques, the following parameters are used: probability of detection (P_D), probability of false alarms (P_{fa}), probability of miss detection (P_{md}), sensing time, and throughput. The simulation results revealed that the HFDI detection method provided sustainable results at low signal-to-noise ratio ranges and improved channel detection and throughput of approximately 17% and 10%, respectively.

Keywords: smart city users; sustainable; 5G technology

Citation: Islam, S.; Budati, A.K.; Hasan, M.K.; Valiveti, H.B.; Vulupala, S.R. Sustainable Non-Cooperative User Detection Techniques in 5G Communications for Smart City Users. *Sustainability* **2023**, *15*, 118. https://doi.org/10.3390/su15010118

Academic Editors: Pradeep Kumar Singh, Dhananjay Singh, Pradip Sharma, Paulo J. Sequeira Gonçalves and Pao-Ann Hsiung

Received: 2 November 2022
Revised: 15 December 2022
Accepted: 16 December 2022
Published: 21 December 2022

1. Introduction

A smart city is an urban area wherein various electronic devices and sensors are installed to facilitate the collection and sharing of information. Most contemporary smart cities rely on 5G technology to share information between networks. The 5G ultra-dense wireless networks can reduce load on converged cell-less communications. Vertically converged architectures are used at access points to enable 5G converged communication. Software-defined radio access networks are used to manage traffic in 5G [1].

Accurate information about spectrum slot availability is needed to carry the data traffic successfully from source to destination without interference to 5G users within a shorter sensing time. This research work is proposed to detect such spectrum slots more accurately within a shorter sensing time.

To estimate the probability of sensing time and channel workload, the authors used window-based and sample-based sensing mechanisms in the CR spectrum. The performance of both sensing techniques is estimated using mean square error with packet distribution. Sensing time and channel workloads are measured as the spectrum usable duration probability and spectrum band used time, respectively. Along with that, switching delay is also measured for specific threshold levels [2]. Spectrum is a scarce resource, and it is a critical task to assign the frequency spectrum slot to smart city users. The authors proposed multiple antenna techniques on energy detection spectrum sensing

to check/detect the spectrum availability in the CR spectrum. The performance of the proposed method is estimated for the licensed users (PU) using the parameters such as P_D, signal to noise ratio (SNR), and multipath fading under the conditions of fast and slow moving signals [3]. The authors proposed a spectrum sensing technique using the sequential approach for the CR-based Internet of Things. Because of the non-sequential approach, the throughput is decreased in the CR spectrum. Dempster–Shafer's theory with n out of n fusion rules is applied in a sequential approach to analyze the performance of the throughput in the spectrum. The results show a significant improvement in P_D, P_{fa}, and overall throughput [4]. The authors proposed their research on throughput with sensing time using a cooperative spectrum sensing technique in CR. The performance is analyzed for the following conditions: OR, AND hard combining rule and equal gain soft combining rules with uniform Gaussian distribution condition. The simulation results are presented between P_D and SNR, throughput, and sensing time [5]. The authors proposed a cyclostationary spectrum sensing technique at different cycle frequencies (CF) to detect the spectrum slot availability at uniform additive white Gaussian noise. The detection process is done to allocate the vacated slot to SUs with fast detection and simple implementation using single-cycle cyclostationary detection. The performance is analyzed with P_D, P_{fa}, and throughput parameters by varying deflection coefficient probability [6].

In Section 2, we present a brief literature review of various spectrum sensing techniques and the importance of spectrum sensing in smart cities.

The paper is organized as follows. Section 2 presents the literature review of spectrum sensing, Section 3 discusses the three detection methods with sensing time and throughput, Section 4 analyzes the results of these methods, and Section 5 presents the conclusions of the study.

2. Literature Review

To identify spectrum availability in the CR, spectrum sensing (SS) techniques are used. Various studies have investigated different SS techniques in half and full duplex paradigms. In full duplex mode, throughput and collision point of view are investigated. The sensing data are most useful for IoT applications and wireless sensor networks [7–9]. There are two types of sensing techniques, cooperative and non-cooperative detection. Spectrum utilization for 5G and beyond communications has also been discussed in detail. Additional features are identified using SS with available channels and free space transmission information [10]. Unused frequency bands/slots in the RF spectrum can be identified by SS only. SS can detect and identify whether the primary users (PU)/licensed users or secondary users (SU)/unlicensed users are utilizing these bands. Compressive sensing frameworks and sparse structures are useful for improving the efficiency of RF spectrum detection in CR. Cooperative detection techniques contain fusion centers to collect sensing data and make decisions about spectrum slot availability based on the threshold value. In case of non-cooperative detection, there is no fusion center, and the spectrum decision is taken care of by itself. Studies have provided examples of how SS can be used with IoT for smart city applications, and they have presented the associated challenges and investigated compressive spectrum sensing techniques [11]. The issues and challenges faced by smart city users include transferring information using wireless devices and networks. CR networks provide solutions for some of the challenges in frequency envelope modulation (FEM) and ad hoc networks. Smart cities need advanced control and excellent networks with the latest infrastructure to provide efficient network services. Challenges in radio spectrum assigning for smart city users in CR networks have also been discussed. Apart from SS, spectrum sharing, decision, and mobility issues have also been discussed with physical and medium access control [12]. In cognitive wireless networks (CWNs), SS was used for efficient multi-node cooperative spectrum sensing (CSS) for applications in smart cities. To improve the reliability and energy efficiency of the spectrum, high computation costs are required for CSS. To ensure efficient utilization of SS, node interpretation should be enhanced and the associated challenges should be addressed. Energy detection (ED)

techniques are useful for minimizing the complexity and optimizing the energy for sensor selection for SS applications. Blockchain encryption is used for storing information in the FC. It is compared with existing approaches, and it was shown that the efficiency improved by 10% by varying the nodes [13]. To develop the city as smart city spectrum is a scarce resource and critical task to identify the frequency availability. Frequency spectrum availability in latest 5G networks can be determined using SS techniques. Various detection techniques have been proposed to improve PU detection in CR networks. The detection performance is estimated by using ED along with various detection criteria. The authors identified PU instead of fast-moving users in the spectrum. The performance of the detection technique was estimated basis parameters such as SNR, PD, number of samples, and fading techniques. There are several issues in wireless communication; computational speed has been improved by adopting artificial intelligence (AI) in wireless communication. There have been several technological advances in 5G supported gadgets, and to meet the networking standards, emerging AI technology is needed. CR is the backbone technology for 5G intelligent radio. Radio spectrum management is required to balance the usage of 5G gadgets in the spectrum. Researchers have focused on various energy efficient SS schemes to identify the frequency spectrum slots available by using cooperative and non-cooperative detection methods [14].

A smart sustainable city is an innovative city that uses various ICTs to improve quality of life, efficiency of urban operations and services, and competitiveness, while ensuring that it meets the needs of present and future generations considering various economic, social, environmental, and cultural aspects. The methods proposed herein can increase the quality of life for smart city users by providing efficient, reliable, and high data transmission spectrum in 5G networks. To provide this service, a sustainable (the ability to be maintained at a certain rate or level) spectrum sensing detection algorithm is needed to determine whether the spectrum is free or occupied.

In existing research, three non-cooperative detection algorithms (MFDI, CFDI, and HFDI) have been proposed that exhibit excellent performance and use GLRT and NP observer detection criteria. However, no contemporary studies have focused on the level of sustainability of these detection methods. In this study, we investigated the range of these three detection methods for producing sustainable results at low SNR regimes. In addition to the three parameters P_D, P_{fa}, and P_{md}, we estimated sensing time and throughput for estimation of sustainability of these detection methods. In Section 3, the three detection methods are presented and the dynamic threshold is formulated, and the equations for the sensing time and throughput are further formulated.

3. Materials and Methods

To determine whether a channel is free or busy, the spectrum hypothesis assumes that only noise is present or both users and noise are present. These hypotheses are represented as Equation (1) [15]:

$$H_o = y(n) = w(n) \tag{1}$$

$$H_1 = y(n) = s(n) + w(n) \tag{2}$$

where H_0 denotes the condition in which the spectrum hole is empty or vacant and only additive white Gaussian noise (AWGN) *w(n)* is exhibited in the spectrum. User presence in the spectrum hole or slot is the scenario is designated as H_1. Here, the original signal is represented by *s(n)*, and the noise signal is *w(n)*. In wireless communication, various noise levels are considered to exist on each channel. Therefore, the threshold for each power/SNR level must be estimated, and the threshold changes dynamically dependent on the received SNR. To estimate the threshold for each channel, the "N" jointly Gaussian random variable is given as Equation (2) [16]:

$$P(y; H_i) = \frac{1}{(2\pi\sigma^2)^{N/2}\det(C)^{1/2}} \exp\left[-\frac{1}{2}(y - H_i)^T C^{-1}(y - H_i)\right] \tag{3}$$

where C^{-1} is the inverse covariance, T is the transpose of the signal, and $H_i = H_0$ and H_1. Additionally, 5G spectrum bands are almost nearest to the satellite frequency bands, i.e., tens of GHz frequency. To estimate the threshold value in the 5G spectrum for user presence and absence in the spectrum, NP detection criteria were used. The NP threshold estimation condition was expressed using Equation (4) [17]:

$$L(Y) = \frac{\left(P(y;H_1)/\sigma^2\right)^2}{\left(P(y;H_0)/\sigma^2\right)^2} = \gamma \tag{4}$$

i. MFDI:

The threshold value in the decision-making device determines how the matched Filter will be used to make decisions. There are near-end and far-end consumers in the cellular radio ecosystem. High-SNR signals are received by near-end users, whereas signals for low SNR are received by far-end users. Estimating user presence under the cellular spectrum threshold is a vital parameter [18–21]. If a static and high threshold value is taken, then at low SNR, no user can be detected, i.e., P_{fa}. In contrast, if a low threshold value is taken, then the strong noise signals cross the threshold, indicating the user's presence, i.e., P_{md}. Therefore, a crucial factor in effectively identifying user presence is threshold estimate. For user identification, we developed a dynamic threshold estimation equation. When determining the ideal threshold value, the detection criteria are crucial. The best threshold value is determined in this study using the NP detection criteria [22–25]. The fading conditions and propagation path losses vary for different users. To estimate the dynamic threshold, a non-uniform AWGN is considered. The received signal is applied to analog to digital converter to convert the analog signal into digital format. The digital signal x(n) is applied as input to the matched filter, as shown in Figure 1. The matched filter maximizes the signal and suppresses the noise. The output of matched filter y(n) is applied to NP for estimation of the threshold. The threshold condition for the MFDI with NP (MFDINP) is given using Equation (5) [26]:

$$L(Y) = (H_1 - H_0)^T C^{-1} y \gtrless \sigma^2 ln(\sqrt{\gamma}) + \frac{1}{2}((H_1 - H_0)^T C^{-1}(H_0 + H_1)) \tag{5}$$

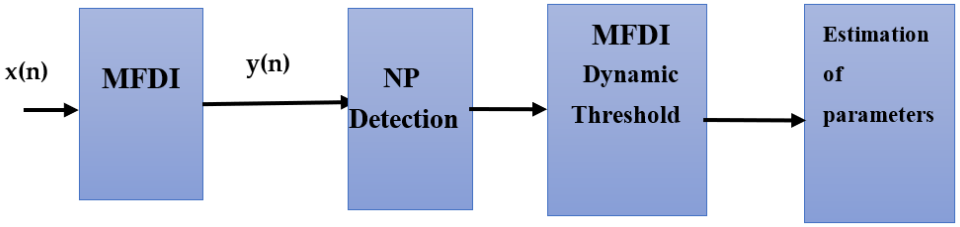

Figure 1. MFDI spectrum sensing technique.

ii. CFDI:

The received signal *y(n)* is given as input to the N-point FFT in the proposed CFDI method, as shown in Figure 2. The FFT is used to determine the frequency content of a signal to perform the spectral analysis in a discrete form. FFT has been used to achieve computational efficiency by adopting a divide-and-conquer approach. A correlator is used to correlate the value of the current sample with that of the preceding sample using the FFT signal output. If the choice matches that of the prior sample, it is regarded as the current sample. If the threshold comparison does not match, the current sample is sent. The threshold condition for the CFDI with NP (CFDINP) is given using Equation (6) [27]:

$$R^{\alpha}_{yy*} = (H_1 - H_0)^T C^{-1} y \gtrless [\sigma^2 \ln(\sqrt{\gamma}) + \frac{1}{2}((H_1 - H_0)^T C^{-1}(H_0 + H_1)) \exp(-j2\pi\alpha n f_s)]^{1/2} \tag{6}$$

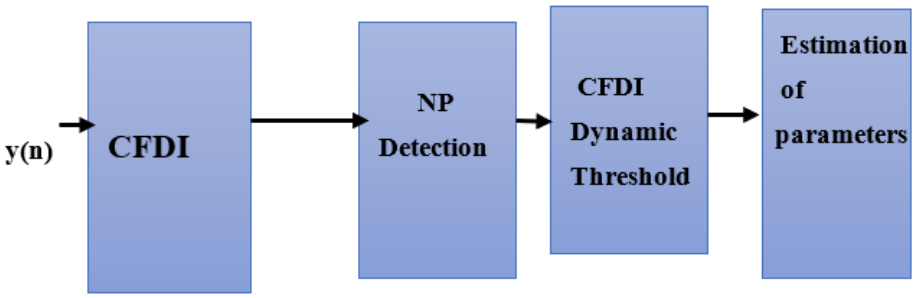

Figure 2. CFDI Spectrum Sensing Technique.

iii. HFDI:

In CFDI, the unfiltered input sample of the received signal was applied directly to the N-point FFT [28]. Due to the unfiltered input signal, P_D might be low at the detection level. The matched filter (MF) increases the signal component at some instant and suppresses the noise amplitude simultaneously. In this study, we combined two detection algorithms, MFDI and CFDI, to form HFDI. The proposed HFDI block diagram is shown in Figure 3.

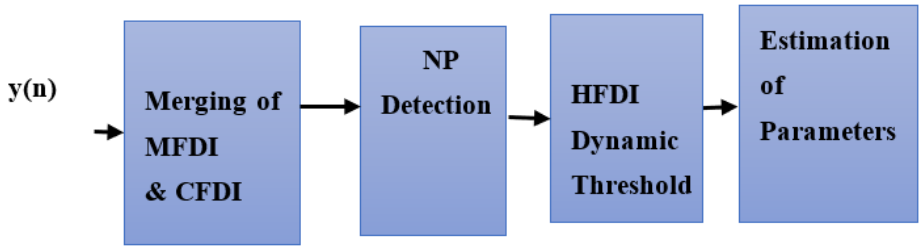

Figure 3. HFDI Spectrum Sensing Technique.

The samples received by the HFDI receiver were applied to MF as *y(n)*. At some point in time, the MF would enhance the signal component while decreasing the noise amplitude. The input of N-point FFT was the output of MF. The frequency domain signal from the output of FFT was also applied to a correlator. The correlator compared previous samples to the results of the N-point FFT [29]. The earlier decision was regarded as the decision for the current iteration if fresh samples were in agreement with the older ones. If the new samples were not correlated, then the samples were given to a threshold detector for comparison. The dynamic threshold was computed for the proposed HFDI using NP detection criteria (HFDINP) (Equation (7)) [30]:

$$L(Y) = \frac{(H_1 - H_0)}{\sigma^2} * [\sigma^2 \ln(\sqrt{\gamma}) + (\frac{1}{2}(H_1 - H_0)^T C^{-1}(H_1 + H_0)) \exp(-j2\pi\alpha n f_s)] \quad (7)$$

To analyze the performance of the detection system, the following parameters were considered [30].

During SS, the channel/sample energy was detected and given to the comparator for checking the threshold level. If the detected sample energy was above the threshold level, the user was presented in the spectrum slot. If the sample energy was less than the threshold level, the spectrum was identified as vacant. Threshold level played a vital role in identifying user presence in the spectrum. Accurate information was estimated for the spectrum by the parameter P_D. Hence, P_D was estimated using Equation (8):

$$P_D = Q[Q^{-1}(P_{fa}) - \sqrt{(H_1 - H_0)^T C^{-1}(H_1 - H_0)}] \quad (8)$$

If the user was located far away from the cell tower or in the overlay region, weak signal was received, and SNR value was almost negative decibels. At low SNR, noise domination was increased or the noise signal energy was higher than the original signal

power. In this case, the threshold value was low, the strongly noise dominated signal crossed the threshold, and the decision was made that the user was present; however, there was no user. This type of wrong detection is called probability of false alarms. These false alarms are estimated using Equation (9):

$$P_{fa} = Q\left(\frac{\gamma - (H_1 - H_0)^T C^{-1} H_0}{\sqrt{(H_1 - H_0)^T C^{-1} (H_1 - H_0)}}\right) \tag{9}$$

If the user was located far away from the cell tower or in the overlay region, weak signal was received and the SNR value was almost negative decibels. At low SNR, the noise domination was increased or the noise signal energy was higher than the original signal power. In this case, the threshold value was high, the signal did not cross the threshold, and the decision was made that the user was absent; however, there were no users. Such wrong detections are called probability of missed detection and are estimated using Equation (10):

$$P_{md} = Q\left(\frac{\gamma - (H_1 - H_0)^T C^{-1} H_1}{\sqrt{(H_1 - H_0)^T C^{-1} (H_1 - H_0)}}\right) \tag{10}$$

Throughput is an important parameter, which also depends on SS. Throughput improvement depends on how much less time is taken by the SS and how much more time is given for the data transmission. In this study, we considered both PU and SU. As shown in Figure 4, T_F is the frame duration, T_S is the sensing the channel time, T_c is the time taken for sensed information given to the fusion center to make decisions or for management of information, and T is the total sensing and decision time of the spectrum. Thus, the data transmission duration was $T_F - (T_s + T_c)$. The throughput estimation with respect to a false alarm is given using Equations (11) and (12):

$$T_{hf} = \frac{T_F - T}{T}\left(1 - P_{fa}\right) \tag{11}$$

$$T_{hd} = \frac{T_F - T}{T}(1 - P_D) \tag{12}$$

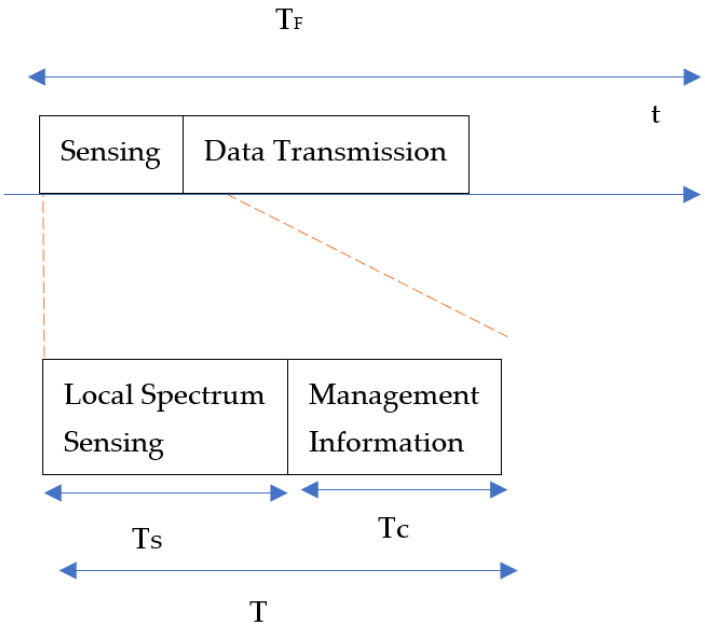

Figure 4. Spectrum sensing time representation.

Data were not continuously transmitted in the spectrum when the spectrum was scanning, and data transmission had to be in the ideal mode. Therefore, a time interval in the data transmission was represented as β. The length of the frame transmitted in the spectrum was represented as T_{RF}.

$$T_{hf1} = \frac{T_F - T}{T}\left(1 - P_{fa}\right)e^{\left(-\frac{T_{RF}}{\beta}\right)} \tag{13}$$

$$T_{hd1} = \frac{T_F - T}{T}(1 - P_D)e^{\left(-\frac{T_{RF}}{\beta}\right)} \tag{14}$$

4. Results

The comparison of the three proposed methods with the parameter P_D is shown in Figure 5. When the power level increased from −10 dB to 0 dB, the detection probability also increased. The best detection method identified the high P_D at low SNR values. At power level of −10 dB, the detection probabilities were 0.45, 0.66, and 0.69 for CFDINP, MFDINP, and HFDINP, respectively, and the proposed HFDINP exhibited better detection than the other two methods. HFDINP and MFDINP provided high detection probability as power level decreased from 1 to −4 dB, but CFDINP offered −1 dB.

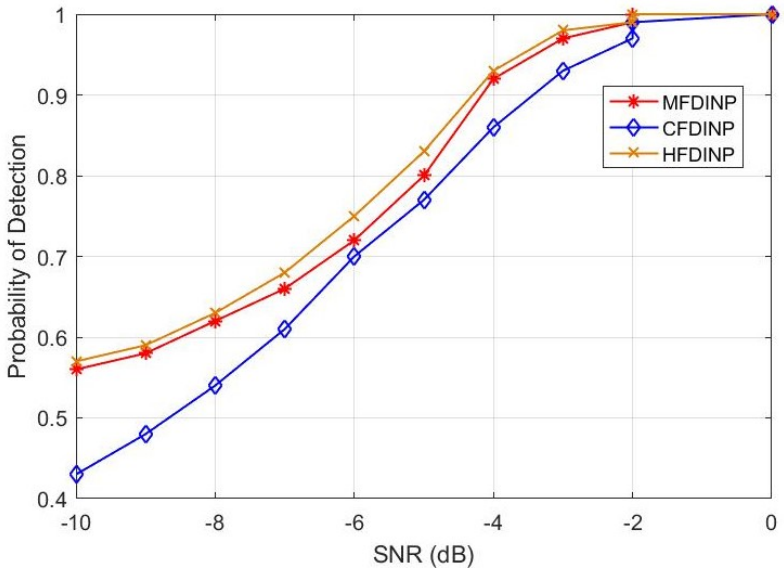

Figure 5. Comparison of P_D vs input SNR.

4.1. Probability of Detection (P_D)

To compare high detection probability, the HFDINP and MFDINP perform better detection than CFDINP at low SNR values. To identify the better detection method out of HFDINP and MFDINP, from the power level −10 dB to −4 dB, HFDINP gave a higher detection probability than MFDINP at all SNR values. The proposed HFDINP exhibited better detection performance than the other two proposed methods. The rate of increase of detection probability between the proposed three methods is analyzed in Figure 6.

If the threshold value is not identified accurately, then there is a provision to acquire low detection probability. If the threshold level changes according to the input SNR, then the detection probability contributes better improvement than the fixed threshold. The fixed and dynamic threshold were compared in terms of P_D for the three proposed methods, and the dynamic threshold was found to provide better solutions for accurate detection. In case of dynamic threshold, the three proposed methods MFDINP, CFDINP, and HFDINP exhibited better detection performance than contemporary methods. As shown in Figure 6, we attempted to identify the better detection algorithm by analyzing the rate of increase of detection probability from −10 dB to −5 dB. At power level of −10 dB, the detection

probabilities of HFDINP, MFDINP, and CFDINP were 0.69, 0.66, and 0.45, respectively. At power level of −5 dB, the detection probabilities of HFDINP, MFDINP, and CFDINP were 0.98, 0.94, and 0.83, respectively. When the power level increased from −10 dB to −5 dB, the rate of increase of detection probability for HFDINP, MFDINP, and CFDINP was 0.29, 0.28, and 0.38, respectively. CFDINP had the highest rate of increase of detection probability than the other two proposed methods, but the detection probabilities were decreased at low SNR levels. HFDINP had higher detection probabilities than the other two proposed methods, even though the rate of detection probability was higher than that of MFDINP and lower than that of CFDINP. HFDINP had higher detection probabilities at a low SNR level than the other two. Hence, HFDINP was the better detection method at low SNR values in case of P_D.

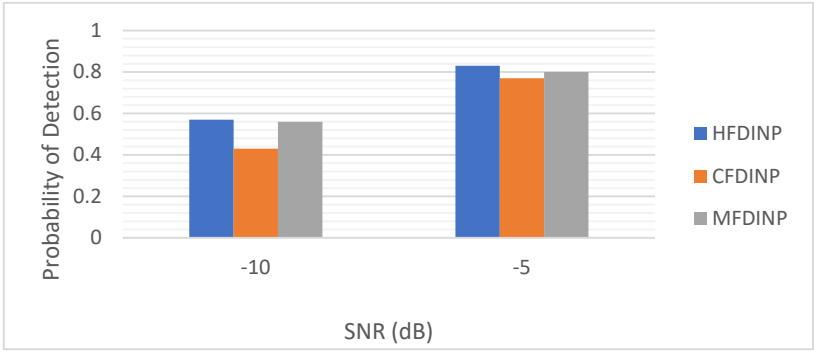

Figure 6. Comparison of P_D with dynamic thresholds.

4.2. Probability of False Alarm (P_{fa})

The three proposed methods are compared in terms of parameter P_{fa} (Figure 7). False alarm probability decreased when the power level increased from −10 dB to 0 dB. Low false alarm probability at low SNR values implies the best performance. At power level of −10 dB, the false alarm probabilities were 0.48, 0.33, and 0.30 for CFDINP, MFDINP, and HFDINP, respectively. At power level of −10 dB, the proposed HFDINP offered less false alarm probability than the other two methods. HFDINP and MFDINP contributed to almost zero false alarms from −4 dB onwards, but CFDINP offered the minimum false alarm probability of 0.02 at 0 dB. The comparison of the three proposed methods also showed that the HFDINP and MFDINP contributed fewer false alarms than CFDINP at low SNR values. To identify the better detection method out of HFDINP and MFDINP, from the power level −10 dB to −4 dB, HFDINP offered less false alarms than MFDINP at all SNR values.

HFDINP exhibited better detection performance than the other two methods at low SNR values. The rate of decrease in false alarm probability of the three proposed methods is compared in Figure 8. If the fixed threshold value was considered low, then there was a chance to get high false alarms. If the threshold level was changed according to the input SNR, then the false alarms mitigated the fixed threshold. The fixed and dynamic threshold were compared for the parameter P_{fa} for the three methods. The dynamic threshold provided a better solution for accurate detection. In case of dynamic threshold, MFDINP, CFDINP, and HFDINP exhibited better detection performance than other contemporary methods. Figure 8 compares the performance of the three proposed methods on the performance factor P_{fa}; it also identifies the better detection algorithm to analyze the rate of decrease of false alarm probability from −10 dB to −5 dB. At power level of −10 dB, the false alarm probabilities of HFDINP, MFDINP, and CFDINP were 0.30, 0.33, and 0.48, respectively. At power level of −5 dB, the false alarm probabilities of HFDINP, MFDINP, and CFDINP were 0.01, 0.05, and 0.22, respectively. When the power level was increased from −10 dB to −5 dB, the rates of decrease of false alarm probability for HFDINP, MFDINP, and CFDINP were 0.29, 0.28, and 0.26, respectively.

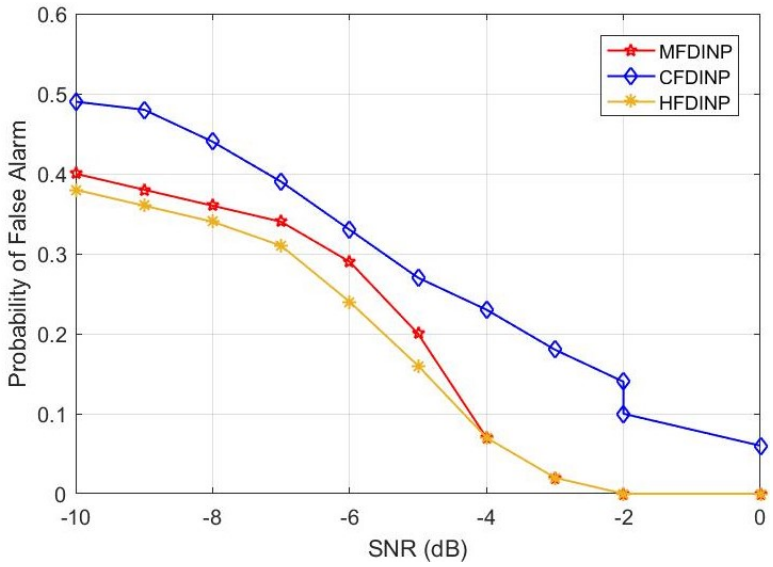

Figure 7. Comparison of P_{fa} vs input SNR.

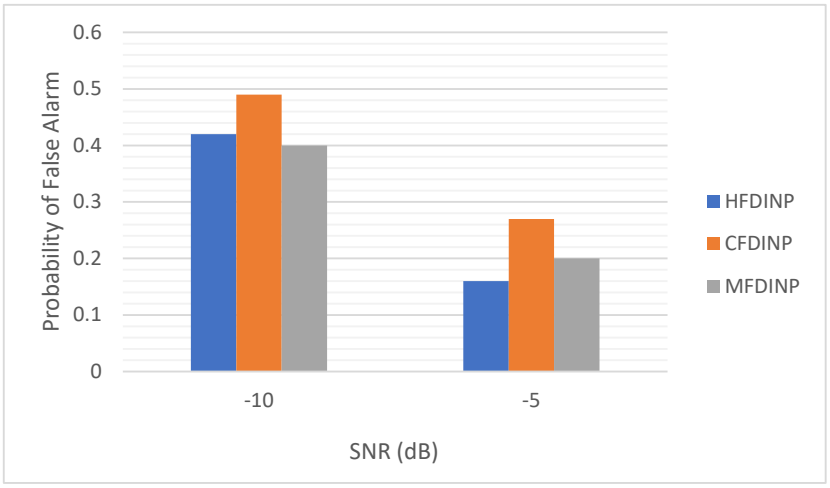

Figure 8. Comparison of P_{fa} with dynamic thresholds.

HFDINP had a higher rate of decrease of P_{fa} than the other two algorithms, and the false alarm probabilities were lower at low SNR levels. At a low SNR level, HFDINP showed better improvement in false alarm probability than the other two methods. Hence, HFDINP was a better detection method at lower SNR values for the parameter P_{fa}.

4.3. Probability of Miss Detection (P_{md})

Comparison of the three proposed methods for parameter Pmd is shown in Figure 9. As power level increased from −10 dB to 0 dB, the missed detection probability decreased. The best detection method is identified as the detection method that offers the lowest probability of missed detection at low SNR values. At power level of −10 dB, the probability of missed detections was 0.54, 0.40, and 0.37 for CFDINP, MFDINP, and HFDINP, respectively. At power level of −10 dB, HFDINP contributed lower missed detection probabilities than the other two methods. HFDINP and MFDINP had almost zero miss detections from −4 dB onwards, and CFDINP offered zero missed detection probability from −1 dB onwards.

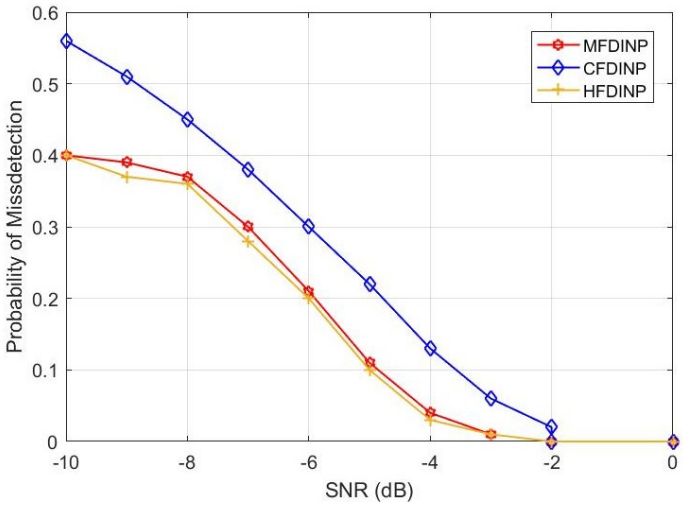

Figure 9. Comparison of P_{md} vs input SNR.

HFDINP and MFDINP provided less missed detection than CFDINP at low SNR values. To identify the better detection method out of HFDINP and MFDINP, for power level from −10 dB to −4 dB, HFDINP contributed less missed detection than MFDINP at all SNR values. HFDINP provided better detection than the other two methods. The rate of decrease of miss detection probability between the proposed three methods was analyzed, as shown in Figure 10. If a high fixed threshold value was considered, there was a possibility of high probability of missed detection. If the threshold level was changed according to the input SNR, the missed detections mitigated the fixed threshold. The fixed and dynamic threshold with parameter P_{md} was compared for the three proposed methods and the dynamic threshold was determined to be the better solution for accurate detection. In dynamic threshold, MFDINP, CFDINP, and HFDINP offered less missed detection than other contemporary methods. The performance was analyzed for the proposed methods by the performance factor P_{md}, as shown in Figure 10.

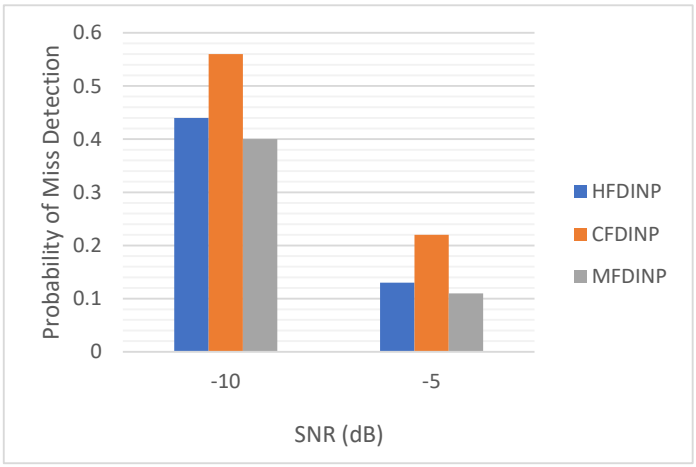

Figure 10. Comparison of P_{md} with dynamic thresholds.

From Figure 10, we attempted to identify the better detection algorithm by analyzing the rate of decrease of missed detection probability from −10 dB to −5 dB. At power level of −10 dB, the missed detection probabilities of HFDINP, MFDINP, and CFDINP were 0.37, 0.40, and 0.54, respectively. At power level of −5 dB, the missed detection probabilities of HFDINP, MFDINP, and CFDINP were 0.01, 0.02, and 0.16, respectively. When the power level increased from −10 dB to −5 dB, the rates of decrease of P_{md} for HFDINP, MFDINP, and CFDINP were 0.36, 0.38, and 0.38, respectively. MFDINP and CFDINP had the same

rates of decrease of missed detection as HFDINP. However, at a low SNR level, HFDINP had fewer miss detection probabilities than the other two methods. HFDINP showed better improvement in missed detection probability at a low SNR level than the other two methods. Hence, HFDINP is a better detection method at low SNR values for the probability of missed detection.

Figure 11 represents the sensing time in milliseconds versus the probability of a false alarm at an SNR of −10 dB. We estimated the sensing time for the three proposed detection techniques. HFDINP required less sensing time than the other two detection techniques. The time saved was 0.01 ms compared with MFDINP and 0.02 ms compared with CFDINP at P_{fa} = 0.1.

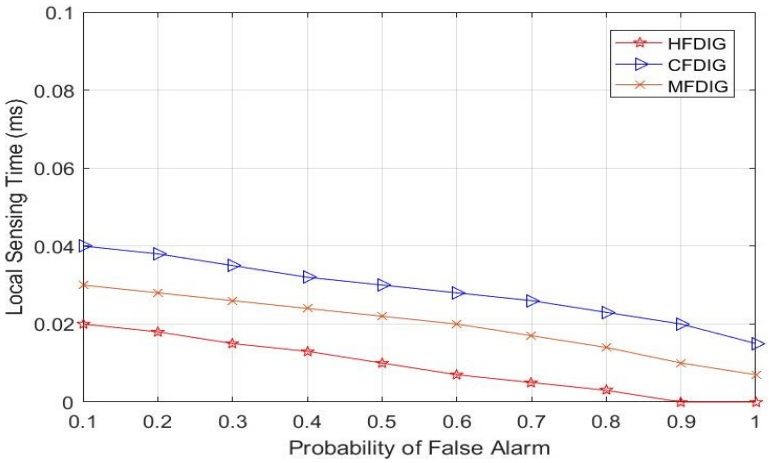

Figure 11. Local sensing time versus probability of false alarm at SNR= −10 dB.

Figure 12 represents the sensing time in milliseconds versus the probability of detection at SNR of −10 dB. HFDINP required less sensing time than the other two detection techniques. The time saved was 0.1 ms and 0.14 ms compared with MFDINP and CFDINP, respectively, at P_D = 1.

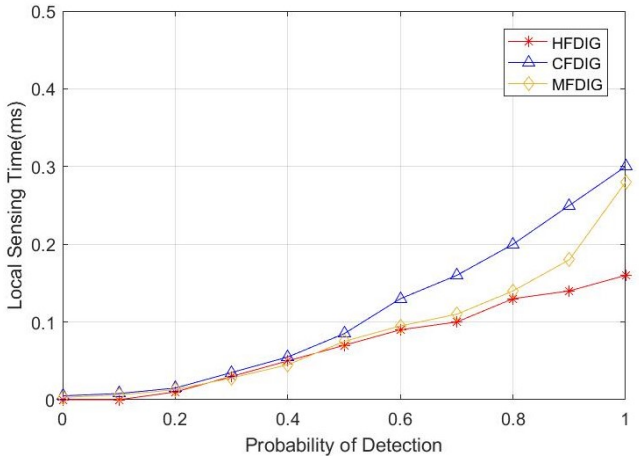

Figure 12. Local sensing time versus probability of detection at SNR = −10 dB.

Figure 13 represents the normalized throughput versus the probability of false alarm for various beta (β) values. β represents data transmission time. As P_{fa} increased, the value of β exponentially decayed, as shown in Equation (13). As shown in Figure 13, the value of β at 500 ms provided better throughput than at 400 ms and 450 ms. Thus, high value of β implies higher throughput.

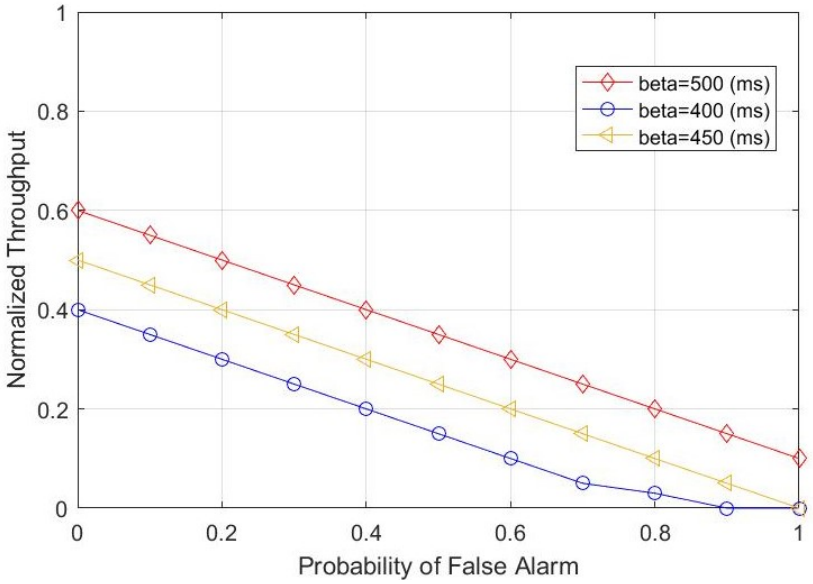

Figure 13. Normalized throughput versus probability of false alarm.

5. Conclusions

Performance analysis was carried out between the three non-cooperative detection methods of HFDINP, MFDINP, and CFDINP based on the parameters P_D, P_{fa}, P_{md}, local sensing time, and throughput. HFDINP provided better sensing performance than the remaining two detection criteria in terms of P_D, P_{fa}, and P_{md}. From these results, HFDINP was identified as the better detection method. To identify SNR values for which HFDINP provided sustainable results, local sensing time and throughput were measured. Under any robust environment, the detection performance should provide sustainable results; thus, to estimate the sustainable performance of HFDINP, sensing time and throughput parameters were considered. HFDINP required less sensing time to scan the spectrum and identify the vacated slots. It required approximately 15% and 12% less time compared to CFDINP and MFDINP at $P_D = 1$. Throughput was high when the value of β was 500 ms compared with that at 450 ms and 400 ms. The three detection methods thus provided better results up to the SNR of −20 dB only.

Author Contributions: Conceptualization, M.K.H.; Methodology, A.K.B. and S.R.V.; Validation, A.K.B.; Investigation, S.I.; Resources, M.K.H.; Writing—original draft, A.K.B.; Writing—review & editing, H.B.V.; Visualization, H.B.V. and S.R.V.; Supervision, S.I. All authors have read and agreed to the published version of the manuscript.

Funding: There is no funding for this research paper.

Institutional Review Board Statement: Not applicable.

Informed Consent Statement: Not applicable.

Data Availability Statement: Not applicable.

Conflicts of Interest: The authors declare no conflict of interest.

References

1. Han, T.; Ge, X.; Wang, L.; Kwak, K.S.; Han, Y.; Liu, X. 5G converged cell-less communications in smart cities. *IEEE Commun. Mag.* **2017**, *55*, 44–50. [CrossRef]
2. Soltani, M.; Baykas, T.; Arslan, H. On reducing multiband spectrum sensing duration for cognitive radio networks. In Proceedings of the 2016 IEEE 84th Vehicular Technology Conference (VTC-Fall), Montreal, QC, Canada, 18–21 September 2016; pp. 1–5.
3. Dhope, T.S.; Simunic, D. Spectrum sensing from smart city perceptive. In Proceedings of the 2018 41st International Convention on Information and Communication Technology, Electronics and Microelectronics (MIPRO), Opatija, Croatia, 21–25 May 2018; pp. 0405–0410.

4. Miah, M.S.; Schukat, M.; Barrett, E. A throughput analysis of an energy-efficient spectrum sensing scheme for the cognitive radio-based Internet of things. *EURASIP J. Wirel. Commun. Netw.* **2021**, 201. [CrossRef]
5. Teguig, D.; Scheers, B.; Le Nir, V. Throughput optimization for cooperative spectrum sensing in cognitive radio networks. In Proceedings of the 2013 Seventh International Conference on Next Generation Mobile Apps, Services and Technologies, Prague, Czech Republic, 25–27 September 2013; pp. 237–243.
6. Derakhshani, M.; Le-Ngoc, T.; Nasiri-Kenari, M. Efficient cooperative cyclostationary spectrum sensing in cognitive radios at low SNR regimes. *IEEE Trans. Wirel. Commun.* **2011**, *10*, 3754–3764. [CrossRef]
7. Elganimi, T.Y.; Rabie, K.M. Multidimensional Generalized Quadrature Index Modulation for 5G Wireless Communications. In Proceedings of the 2021 IEEE 93rd Vehicular Technology Conference (VTC2021-Spring), Helsinki, Finland, 25–28 April 2021; pp. 1–6.
8. Kansal, L.; Berra, S.; Mounir, M.; Miglani, R.; Dinis, R.; Rabie, K. Performance Analysis of Massive MIMO-OFDM System Incorporated with Various Transforms for Image Communication in 5G Systems. *Electronics* **2022**, *11*, 621. [CrossRef]
9. Tian, X.; Huang, Y.; Verma, S.; Jin, M.; Ghosh, U.; Rabie, K.M.; Do, D.T. Power allocation scheme for maximizing spectral efficiency and energy efficiency tradeoff for uplink NOMA systems in B5G/6G. *Phys. Commun.* **2020**, *43*, 101227. [CrossRef]
10. Nasser, A.; Al Haj Hassan, H.; Abou Chaaya, J.; Mansour, A.; Yao, K.C. Spectrum sensing for cognitive radio: Recent advances and future challenge. *Sensors* **2021**, *21*, 2408. [CrossRef] [PubMed]
11. Benazzouza, S.; Ridouani, M.; Salahdine, F.; Hayar, A. A survey on compressive spectrum sensing for cognitive radio networks. In Proceedings of the 2019 IEEE International Smart Cities Conference (ISC2), Casablanca, Morocco, 14–17 October 2019; pp. 535–541.
12. Cooke, C.D.; Anderson, A.L. Autonomous Radios and Open Spectrum in Smart Cities. In *Smart Cities: Foundations, Principles, and Applications*; Wiley: New York, NY, USA, 2017; pp. 99–123.
13. Rani, S.; Babbar, H.; Shah, S.H.A.; Singh, A. Improvement of energy conservation using blockchain-enabled cognitive wireless networks for smart cities. *Sci. Rep.* **2022**, *12*, 1–10. [CrossRef]
14. Murugan, S.; Sumithra, M.G. Energy Efficient Cognitive Radio Spectrum Sensing for 5G Networks–A Survey. *EAI Endorsed Trans. Energy Web* **2021**, *8*, e8. [CrossRef]
15. Tertinek, S. Optimum Detection of Deterministic and Random Signals. Report Written for the Advanced Signal Processing 1 SE. 2004, pp. 1–6. Available online: https://www2.spsc.tugraz.at/www-archive/AdvancedSignalProcessing/WS04-DSPPrinciples/TertinekPaper.pdf (accessed on 1 November 2022).
16. Gong, S.; Wang, P.; Liu, W. Spectrum sensing under distribution uncertainty in cognitive radio networks. In Proceedings of the 2012 IEEE International Conference on Communications, Ottawa, ON, Canada, 10–15 June 2012; pp. 1512–1516. [CrossRef]
17. Budati, A.K.; Valiveti, H. Identify the user presence by GLRT and NP detection criteria in cognitive radio spectrum sensing. *Int. J. Commun. Syst.* **2022**, *35*, e4142. [CrossRef]
18. Biørn-Hansen, A.; Rieger, C.; Grønli, T.M.; Majchrzak, T.A.; Ghinea, G. An empirical investigation of performance overhead in cross-platform mobile development frameworks. *Empir. Softw. Eng.* **2020**, *25*, 2997–3040. [CrossRef]
19. Zhang, Y.; He, W.; Li, X.; Peng, H.; Rabie, K.M.; Nauryzbayev, G.; ElHalawany, B.M.; Zhu, M. Covert Communication in Downlink NOMA Systems with Channel Uncertainty. *IEEE Sens. J.* **2022**, *22*, 19101–19112. [CrossRef]
20. Liu, H.; Li, G.; Li, X.; Liu, Y.; Huang, G.; Ding, Z. Effective Capacity Analysis of STAR-RIS Assisted NOMA Networks. *IEEE Wirel. Commun. Lett.* **2022**, *11*, 1930–1934. [CrossRef]
21. Li, X.; Gao, X.; Liu, Y.; Huang, G.; Zeng, M.; Qiao, D. Overlay Cognitive Radio-assisted NOMA Intelligent Transportation Systems with Imperfect SIC and CEEs. *Chin. J. Electron.* **2022**, *32*, 1–13. [CrossRef]
22. Yang, L.; Yu, K.; Yang, S.X.; Chakraborty, C.; Lu, Y.; Guo, T. An intelligent trust cloud management method for secure clustering in 5G enabled internet of medical things. *IEEE Trans. Ind. Inform.* **2021**, *18*, 8864–8875. [CrossRef]
23. Chakraborty, C.; Rodrigues, J.J. A comprehensive review on device-to-device communication paradigm: Trends, challenges and applications. *Wirel. Pers. Commun.* **2020**, *114*, 185–207. [CrossRef]
24. Natarajan, M.; Arthi, R.; Murugan, K. Energy aware optimal cluster head selection in wireless sensor networks. In Proceedings of the 2013 Fourth International Conference on Computing, Communications and Networking Technologies (ICCCNT), Tiruchengode, India, 4–6 July 2013; pp. 1–4.
25. Arthi, R.; Rawat, D.S.; Pillai, A.; Nair, Y.; Kausik, S.S. Analysis of indoor localization algorithm for wifi using received signal strength. In *International Conference on Emerging Trends and Advances in Electrical Engineering and Renewable Energy, International Conference on Emerging Trends and Advances in Electrical Engineering and Renewable Energy*; Springer: Singapore, 2021; pp. 423–431.
26. Kumar, B.A.; Hima Bindu, V.; Swetha, N. User Detection Using Cyclostationary Feature Detection in Cognitive Radio Networks with Various Detection Criteria. In *International Conference on Innovative Computing and Communications*; Springer: Singapore, 2021; pp. 1013–1029.
27. Maeda, K.; Benjebbour, A.; Asai, T.; Furuno, T.; Ohya, T. Recognition among OFDM-based systems utilizing cyclostationarity-inducing transmission. In Proceedings of the 2007 2nd IEEE International Symposium on New Frontiers in Dynamic Spectrum Access Networks, Dublin, Ireland, 17–20 April 2007; pp. 516–523.
28. Budati, A.K.; Ghinea, G.; Ganesh, S.N.V. Novel Aninath Computation Detection Algorithm to Identify the UAV Users in 5G Networks. *Wirel. Pers. Commun.* **2022**, *127*, 963–978. [CrossRef]

29. Sharma, S.; Rani, M.; Goyal, S.B. Energy efficient data dissemination with ATIM window and dynamic sink in wireless sensor networks. In Proceedings of the 2009 International Conference on Advances in Recent Technologies in Communication and Computing, Kottayam, India, 27–28 October 2009; pp. 559–564.
30. Chen, W.; Wang, Z.; Ding, D.; Ghinea, G.; Liu, H. Distributed Formation-Containment Control for Discrete-Time Multiagent Systems Under Dynamic Event-Triggered Transmission Scheme. *IEEE Trans. Syst. Man Cybern. Syst.* **2022**. [CrossRef]